JTTEE5 18:555–562
DOI: 10.1007/s11666-009-9345-y
1059-9630/$19.00 © ASM International

Effect of Ceramic Particles on Properties of Cold-Sprayed Ni-20Cr+Al_2O_3 Coatings

Heli Koivuluoto and Petri Vuoristo

(Submitted January 5, 2009; in revised form May 20, 2009)

Cold spraying is a thermal spray process enabling the production of metallic and metal-ceramic coatings with low porosity and low oxygen content, capable of, e.g., resisting corrosion. The aim of this study was to characterize the microstructural and mechanical properties of cold-sprayed Ni-20Cr+Al_2O_3 coatings and to clarify the effect of the hard particles on different coating properties. Accordingly, the research focused on the microstructure, denseness (impermeability), adhesion strength, and hardness of the coatings. Scanning electron microscopy (SEM) analysis and corrosion tests were run to gain information on the through-porosity. Ceramic addition in cold-sprayed Ni-20Cr+Al_2O_3 coatings improved their quality by lowering their porosity. Moreover, hardness was slightly higher than those of cold-sprayed Ni-20Cr coating, indicating a hardening effect by the ceramic particles. The addition of Al_2O_3 also made it possible to use high gas temperatures without nozzle clogging, which affects coating properties, such as coating thickness, denseness, and hardness.

Keywords coating structure, cold spraying, denseness, mechanical properties, Ni-20Cr+Al_2O_3

1. Introduction

Cold spraying, one of the latest thermal spray techniques, developed in the former Soviet Union in the 1980s, is based on lower gas temperatures and higher particle velocities than those encountered in other thermal spray methods (Ref 1). In the cold spray (CS) process, a gas is accelerated to supersonic velocity by a converging-diverging de Laval type nozzle (Ref 2). A coating is formed when powder particles at high velocities (high kinetic energy) impact on the substrate, deform, and adhere to it or to other particles. In addition, good bonding between CS powder particles requires a high plastic deformation during particle impact (Ref 3-5). Powder particles adhere to the substrate in solid form well below the powder melting temperature, and on impact deform and bond together, forming a coating (Ref 3). For successful bonding, deposition conditions should be such that oxide layers on the particle surfaces are fractured during impact (Ref 4). Cold spraying can make use of a wide range of coating and substrate materials, e.g., pure metals, metal alloys, polymers, and composites (Ref 6).

Usually, thermal-sprayed nickel alloy coatings, e.g., nickel chromium alloys, are used for applications requiring resistance to corrosion and oxidation and for repairs and bond coats (Ref 7). Thus, nickel chromium alloy coatings are of high interest to CS because the technique enables the production of metallic and metal-ceramic coatings with low porosity and low oxygen content. In these coatings, denseness (impermeability) is the criterion for good corrosion resistance (Ref 2). CS coatings also show low residual stresses, rather high adhesion, and hardness normally higher than that of the corresponding bulk materials. High hardness is caused by significant work hardening of the sprayed particles (Ref 3). Calla et al. (Ref 8) reported that an increased particle velocity due to an increased driving pressure resulted in more cold working in the coating, leading to high hardness. High velocities also result in a high impact deformation at the interface of both substrate and coating and between particles. Furthermore, gas temperature affects significantly the quality of the CS coatings. A high temperature leads to high velocity and, therefore, to strong impacts. Moreover, because deposition efficiency (DE) depends on the temperature of the gas, DE is reportedly improved at high gas temperatures (Ref 9). The gas temperature affects the gas and particle velocity, meaning higher velocity at higher temperature. Reportedly, increased particle temperature also improves the coating quality in the CS process (Ref 10, 11).

This study sought to investigate the effect of the Al_2O_3 particles on the properties of CS Ni-20Cr+Al_2O_3 coatings. It was found out experimentally some technical spraying limitations to spray Ni-20Cr powder due to the fact that high gas temperatures can cause nozzle clogging with Ni-20Cr particles. To solve such problems, a metallic powder was mixed with a ceramic powder to eliminate clogging and, consequently, to make it possible to use higher gas temperatures. The main function of the Al_2O_3 addition is to keep the nozzle of the gun clean. Furthermore, Al_2O_3 particles activate (clean and roughen) the sprayed surfaces, i.e., through activation the surface becomes cleaner and more adaptive to the sprayed

Heli Koivuluoto and **Petri Vuoristo**, Department of Materials Science, Tampere University of Technology, P.O. Box 589, 33101 Tampere, Finland. Contact e-mail: heli.koivuluoto@tut.fi.

particles, which then stick better to the surface. In addition to these, Al_2O_3 particles mechanically affect the coating by hammering of the substrate/sprayed layers or by the so-called shot peening effect via particle impacts (Ref 12). During the particle impacts, collision of the ceramic particles also increases the deformation of the metallic particles (compacting effect), which affects the coating properties and DE particularly in the low-pressure CS process (Ref 13). In this study, the properties of microstructure, denseness, adhesion strength, and hardness were investigated and three different particle sizes of Al_2O_3 powders and two different compositions of each particle size were tested. The aim of this work was to prepare CS Ni-20Cr+Al_2O_3 coatings with improved properties using higher gas temperatures, which were made possible by spraying Ni-20Cr with a simultaneous Al_2O_3 injection.

2. Experimental Techniques

Ni-20Cr powder was cold-sprayed with different parameters: gas temperatures of 500 °C for Ni-20Cr and 700 °C for Ni-20Cr+Al_2O_3, and with six different metal alloy-ceramic powder mixtures. A gas-atomized, spherical Ni-20Cr powder having a particle size of $-22.5+10$ μm, supplied by H.C. Starck, and as the ceramic addition fused and crushed, irregular, blocky Al_2O_3 powders, also from H.C. Starck were used in this study. Three different particle sizes of Al_2O_3 were tested, $-90+45$ μm, $-45+22$ μm, and $-22+5$ μm, in two different compositions, 50 and 30 vol.%. Grit-blasted (1 mm Al_2O_3) carbon steel sheets ($50 \times 100 \times 1.5$ mm) were used as substrates.

CS coatings were prepared at Linde AG Linde Gas Division (Unterschleissheim, Germany) with a CGT Kinetiks 4000 CS system (high-pressure CS equipment). Spraying parameters for the CS Ni-20Cr+Al_2O_3 and Ni-20Cr coatings are shown in Table 1. All Ni-20Cr+Al_2O_3 powders were sprayed using the same parameters. The CS Ni-20Cr without added Al_2O_3 particles could not be sprayed at high temperature, i.e., at 700 and 600 °C, because powder clogged the nozzle, therefore, the temperature had to be dropped to 500 °C. This is the reason the Ni-20Cr coating was sprayed at 500 °C whereas Ni-20Cr+Al_2O_3 coatings at 700 °C (Al_2O_3 particles made it possible to use higher gas temperature). Furthermore, the reason for the use of the higher gas temperature with the Ni-20Cr+Al_2O_3 powders was that reportedly high temperatures improve the coating quality (Ref 11).

The coatings were characterized using a Philips XL30 scanning electron microscope (SEM). Microstructures of the coatings were studied from unetched metallographic cross section samples, and surfaces were analyzed with a Leica MZ7.5 stereomicroscope (SM). Al_2O_3 fractions were calculated from the coating cross sections using image analysis (ImageJ). Coating thicknesses were measured from cross sections of the coatings as an average of eight measurements, whereas the coating denseness and especially the through-porosity were studied using spray tests and open-cell electrochemical potential measurements. The salt spray test was done according to the ASTM B117 standard. Substrates were masked with epoxy paint before testing in order to allow the coating surfaces to be in contact only with the corroding salt spray. A 5 wt.% NaCl solution was used with an exposure time of 48 h, a temperature of 35-40 °C, a solution pH of 6.3, and a solution accumulation of 0.04 mL/cm^2 h. Surfaces of the coatings were analyzed visually and amounts (%) of corrosion spots were characterized using image analysis (ImageJ). The electrochemical cell used in the open-cell potential measurements consisted of a plastic tube, of diameter 20 mm and volume 12 mL, glued on the surface of the coating specimen. A 3.5 wt.% NaCl solution was placed in the tube for nine-day measurements. Open-cell potential measurements were taken with a Fluke 79 III true RMS multimeter. A silver/silver chloride (Ag/AgCl) electrode was used as a reference electrode. Adhesion strength (standard EN-582) was measured in a tensile test (Instron 1185 mechanical testing machine) as an average of three measurements. Vickers hardness ($HV_{0.3}$) was measured as an average of ten measurements with a Matsuzawa hardness tester.

3. Results and Discussion

Nickel alloys are known for their good corrosion resistance. Furthermore, nickel alloy coatings give protection against wet corrosion to steel substrates that require a fully dense (overall dense) coating. The effect on the coating properties (denseness and mechanical properties) of added Al_2O_3 particles in the Ni-20Cr powder were investigated. The addition of Al_2O_3 powder was studied to decrease the coating porosity and to enable the use of higher gas temperatures.

3.1 Microstructure

The microstructure of a Ni-20Cr coating is shown in Fig. 1. Some pores and defects appear in the coating

Table 1 Spraying parameters of CS Ni-20Cr+Al_2O_3 and CS Ni-20Cr coatings

CS coating	Process gas	Pressure, bar	Gas temperature, °C	N_2 flow rate, m^3/h	Traverse speed, m/min	Number of layers
Ni-20Cr+Al_2O_3	N_2	37	700	82	20	3
Ni-20Cr	N_2	36	500	95	20	3

Spraying distance was 40 mm. Distance between two adjacent spray beads was 1.5 mm

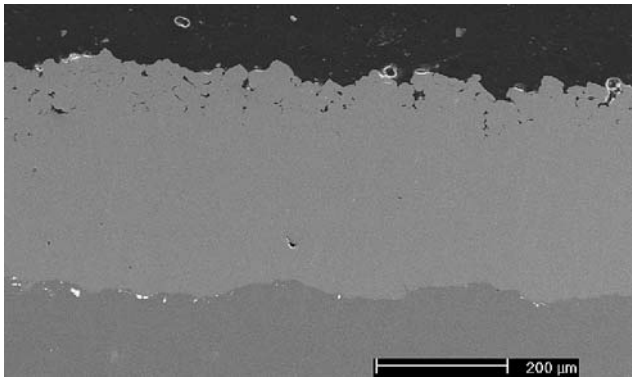

Fig. 1 Microstructure of CS Ni-20Cr coating on grit-blasted steel substrate, SEM image

structure mostly near its surface. It is worth noting that the Ni-20Cr coating without an Al_2O_3 addition was sprayed at a low gas temperature (500 °C). At higher temperatures (600 and 700 °C), the Ni-20Cr powder clogged the nozzle; therefore, 500 °C was the highest gas temperature which could be used in this study without nozzle clogging. At higher temperatures, Ni-20Cr particles were possibly in a soft-state because of thermal softening and thus, easily stuck to the surface of the nozzle whereas the Al_2O_3 particles mixed with Ni-20Cr particles apparently kept the nozzle clean and eliminated clogging. In the powder (metallic-ceramic particle mixture)—gas flow, ceramic particles can prevent metallic particles from sticking inside the nozzle wall at higher preheating temperatures. This arises from the durability of ceramic particles (high hardness and high melting point). Therefore, this study shows the comparison between Ni-20Cr and Ni-20Cr+Al_2O_3 coatings sprayed with the optimal gas temperatures for these coating materials (Ni-20Cr: 500 °C and Ni-20Cr+Al_2O_3: 700 °C).

Figure 2 shows microstructures of Ni-20Cr+Al_2O_3 coatings with Fig. 2(a) and (d) corresponding to an Al_2O_3 particle size of −90 +45 µm, Fig. 2(b) and (e) to a particle size −45 + 22 µm, and Fig. 2(c) and (f) to −22 + 5 µm with both compositions of 50% and 30%, respectively. In the microstructures, the detected dark particles are Al_2O_3. Clearly in the coating, the number of Al_2O_3 particles decreased with the lower Al_2O_3 composition (30%). Furthermore, the coating thickness was greater for the 30% Al_2O_3 composition (see Fig. 3). Table 2 summarizes the comparison between Al_2O_3 fractions in the powder and in the coating using image analysis on the coating cross sections in Fig. 2(a) to (f). The finer the Al_2O_3 particles, the better their chance of developing a velocity high enough to impact on a substrate and stick to its surface or to other particles (Ref 14). However, in some cases though fine particles may have high acceleration velocity, they also rapidly lose it after the nozzle because of bow shock waves (Ref 14). This is a possible reason that the Ni-20Cr+Al_2O_3 (−22 + 5 µm) coating contained lower amount of Al_2O_3 particles in its structure than Ni-20Cr+Al_2O_3 (−45 + 22 µm) coating. In addition, spraying materials have specific ranges of particle size (fine to coarse) at critical velocity (Ref 14). Adding Al_2O_3 particles to the metallic powder could extend the spraying conditions (possibility to use high gas temperature) to improve coating properties (e.g., microstructural properties).

Figure 3 summarizes the thicknesses of the CS Ni-20Cr+Al_2O_3 and Ni-20Cr coatings. Clearly, a higher coating thickness was achieved with less Al_2O_3 (30% instead of 50%) arisen from the initial powder composition. An Al_2O_3 addition improved the metallic deposition buildup (comparison between coating thicknesses and volume amount of metallic particles (100%, 70%, or 50%) in the powder mixtures), suggesting a compacting and peening effect of the hard particles together with an influence of higher gas temperature. This result was achieved with all the metal-ceramic powder mixtures; the best result was obtained with the 30% Al_2O_3 composition. Metallic particles have higher capability to build up the deposition (due to the capability to undergo plastic deformation during impact) than ceramic particles. Thus, powder with higher amount of Ni-20Cr particles (lower amount Al_2O_3) has higher deposition buildup. Moreover, coating thicknesses increased slightly as the Al_2O_3 particles increased in size. This is possible due to the highest compacting effect of Al_2O_3 particles during spraying.

Figure 4 compares the cross section regions near to the surfaces of Ni-20Cr and Ni-20Cr+50Al_2O_3 (−90 + 45 µm) coatings. In Fig. 4(a), the dark areas are pores and in Fig. 4(b) they are mainly Al_2O_3 particles. The Ni-20Cr coating had a porous layer with more open particle boundaries on top, whereas the Ni-20Cr+50Al_2O_3 coating was dense with only a few pores, indicating a densifing effect by the use of Al_2O_3 particles and higher gas temperature.

Adding Al_2O_3 particles to the metallic Ni-20Cr powder was observed to affect the coating's microstructure and thickness. In this study, the most important function of the Al_2O_3 powder was the possibility to use a high gas temperature to obtain a high deposition buildup. Furthermore, the porosity of the Ni-20Cr+Al_2O_3 coatings decreased with a Al_2O_3 addition, as confirmed by SEM examinations. The sprayed surfaces (substrate or previous coating layers) were activated and hammered by Al_2O_3 particles and higher gas temperatures were made possible due to the barrel cleaning action of the Al_2O_3 particles producing a denser coating structure (noticed also in corrosion studies, in Section 3.2).

3.2 Coating Denseness

A salt spray test was run to analyze the denseness of the coatings and the effect of the added Al_2O_3 particles on the protective behavior of Ni-20Cr+Al_2O_3 coatings. A pure Ni-20Cr coating was also tested for reference. Figure 5 shows a SM image of the Ni-20Cr coating surface after a 48-h exposure in a salt spray chamber. The surface was strongly corroded because corrosion products from the substrate could openly diffuse from the coating interface to its surface (through-porosity; *brown areas* in Fig. 5).

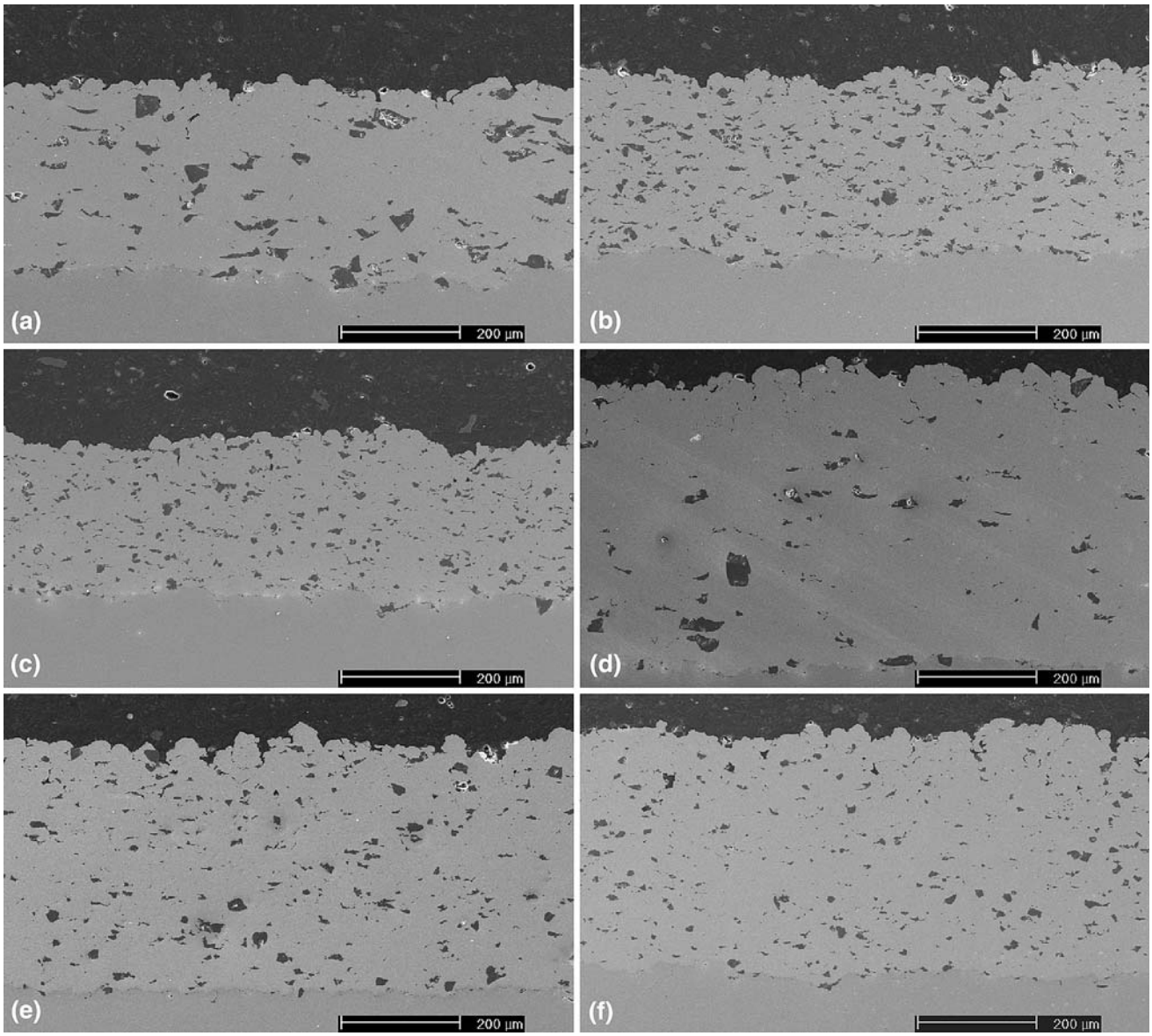

Fig. 2 Microstructure of CS (a) Ni-20Cr+50Al_2O_3 (−90 + 45 μm), (b) Ni-20Cr+50Al_2O_3 (−45 + 22 μm), (c) Ni-20Cr+50Al_2O_3 (−22 + 5 μm), (d) Ni-20Cr+30Al_2O_3 (−90 + 45 μm), (e) Ni-20Cr+30Al_2O_3 (−45 + 22 μm), and (f) Ni-20Cr+30Al_2O_3 (−22 + 5 μm) coatings on grit-blasted steel substrate, SEM images

After 48 h in the salt spray chamber, the Ni-20Cr+Al_2O_3 coatings showed spots of pit corrosion by visual quantification. SM images of Ni-20Cr+Al_2O_3 coating surfaces are shown in Fig. 6. In addition, the Ni-20Cr+30Al_2O_3 exhibited more corrosion spots than the corresponding Ni-20Cr+50Al_2O_3, a behavior observed with all particle sizes of Al_2O_3 powders. A quantitative analysis (%) of corrosion spots on the surfaces of the Ni-20Cr and Ni-20Cr+Al_2O_3 coatings were characterized from Fig. 5 and 6(a) to (f). Results of amount of corrosion areas are 45.5% (Ni-20Cr), 0.8% (Ni-20Cr+50Al_2O_3, −90 + 45 μm), 1.9% (Ni-20Cr+50Al_2O_3, −45 + 22 μm), 3.3% (Ni-20Cr+50Al_2O_3, −22 + 5 μm), 1.7% (Ni-20Cr+30Al_2O_3, −90 + 45 μm), 2.2% (Ni-20Cr+30Al_2O_3, −45 + 22 μm), and 5.2% (Ni-20Cr+30Al_2O_3, −22 + 5 μm). The Ni-20Cr+Al_2O_3 coatings contained less through-porosity than the pure Ni-20Cr coating indicating higher denseness of the Ni-20Cr+Al_2O_3 coating. The through-porosity of the Ni-20Cr+Al_2O_3 coatings decreased with an increasing size of Al_2O_3 particles. On the other hand, the through-porosity of the Ni-20Cr+50Al_2O_3 dropped below that of the 30% composition.

CS coatings were slightly porous (contained through-porosity), a fact that was already shown already in previous corrosion results (Ref 15, 16). Existing porosity (especially through-porosity) is very detrimental to corrosion resistance especially in wet conditions. Salt spray tests and open-cell potential measurements as auxiliary

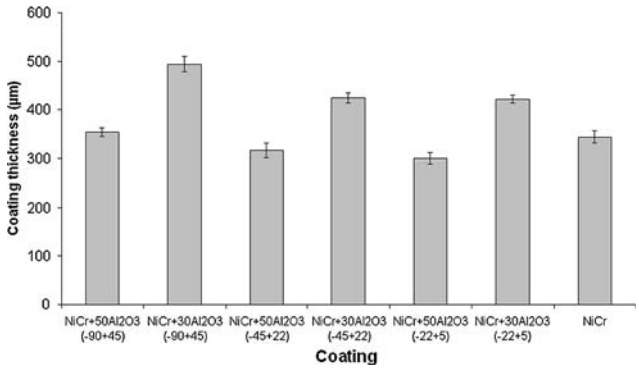

Fig. 3 Thickness (and standard deviations) of CS Ni-20Cr+Al_2O_3 coatings with 30% or 50% Al_2O_3 (Al_2O_3 particle sizes: $-90+45$ µm, $-45+22$ µm, and $-22+5$ µm) and Ni-20Cr coating

Table 2 Fractions of Al_2O_3 particles in the powder and in the CS Ni-20Cr+Al_2O_3 coatings analyzed from cross sections of the coatings by image analysis

Powder/coating	Fraction of Al_2O_3 in the powder, vol.%	Fraction of Al_2O_3 in the coating, vol.%
Ni-20Cr+50Al_2O_3 ($-90+45$ µm)	50	8.2
Ni-20Cr+50Al_2O_3 ($-45+22$ µm)	50	11.2
Ni-20Cr+50Al_2O_3 ($-22+5$ µm)	50	10.1
Ni-20Cr+30Al_2O_3 ($-90+45$ µm)	30	3.6
Ni-20Cr+30Al_2O_3 ($-45+22$ µm)	30	6.4
Ni-20Cr+30Al_2O_3 ($-22+5$ µm)	30	5.2

tests were useful and fast methods to analyze the existing through-porosity in the coating structures. Open-cell potential measurements were taken to identify the existing through-porosity in the Ni-20Cr+Al_2O_3 coatings. The open-cell potential of the substrate material (Fe52) was −700 mV (Ref 16). When open-cell potential of a coating approaches the open-cell potential of the substrate, a salt solution has open access to penetrate from the coating surface into the interface of the coating and the substrate. The effect of an Al_2O_3 addition on the Ni-20Cr+Al_2O_3 coating denseness was tested with open-cell potential measurements. Results are presented in Fig. 7. The open-cell potential of the Ni-20Cr was not measured because of its weak protection in the salt spray test, the two methods being complementary. The open-cell potential measurements showed existing through-porosity in the coatings. Nevertheless, the Ni-20Cr+50Al_2O_3 ($-90+45$ µm) coating showed the fewest weak points after the salt spray test (Fig. 6a) and a slightly higher open-cell potential than the other coatings, indicating a somewhat lower through-porosity.

According to SEM analysis (Figs. 1 and 4a) and the salt spray test (Fig. 5), the Ni-20Cr coating had several weak

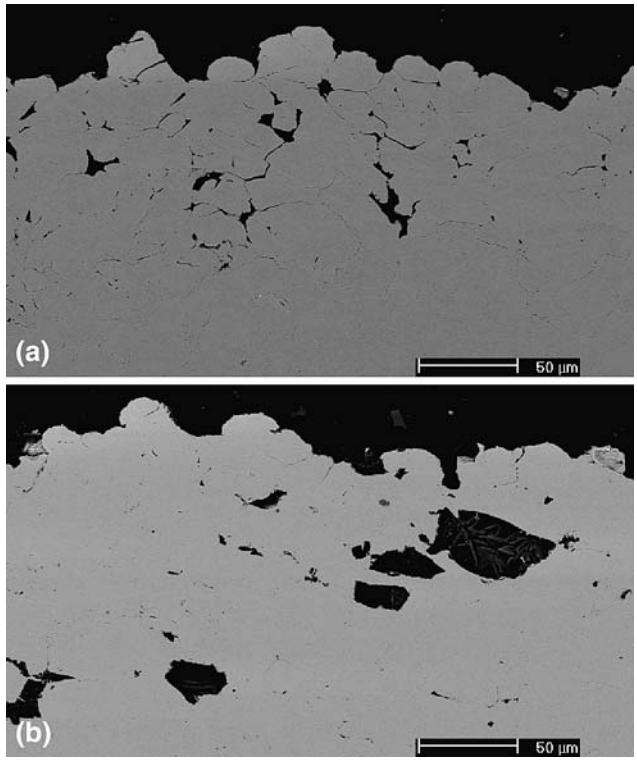

Fig. 4 Coating structure near the surface of CS (a) Ni-20Cr and (b) Ni-20Cr+50Al_2O_3 ($-90+45$ µm) coatings, BSE images (SEM)

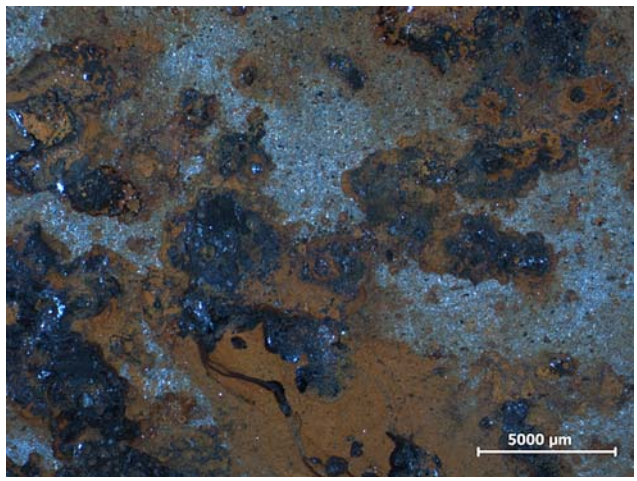

Fig. 5 Strongly corroded surface of CS Ni-20Cr coating after 48-h salt spray test, SM image

points and in addition, the salt spray test showed through-porosity in the coating structure. After the salt spray test, the coating surface was mostly corroded (iron oxide), and the salt solution had penetrated into the interface between the coating and the substrate, indicating an existing through-porosity. In addition, pores and especially a porous layer near the surface were evident in the SEM images. Compared to the Ni-20Cr coating, the

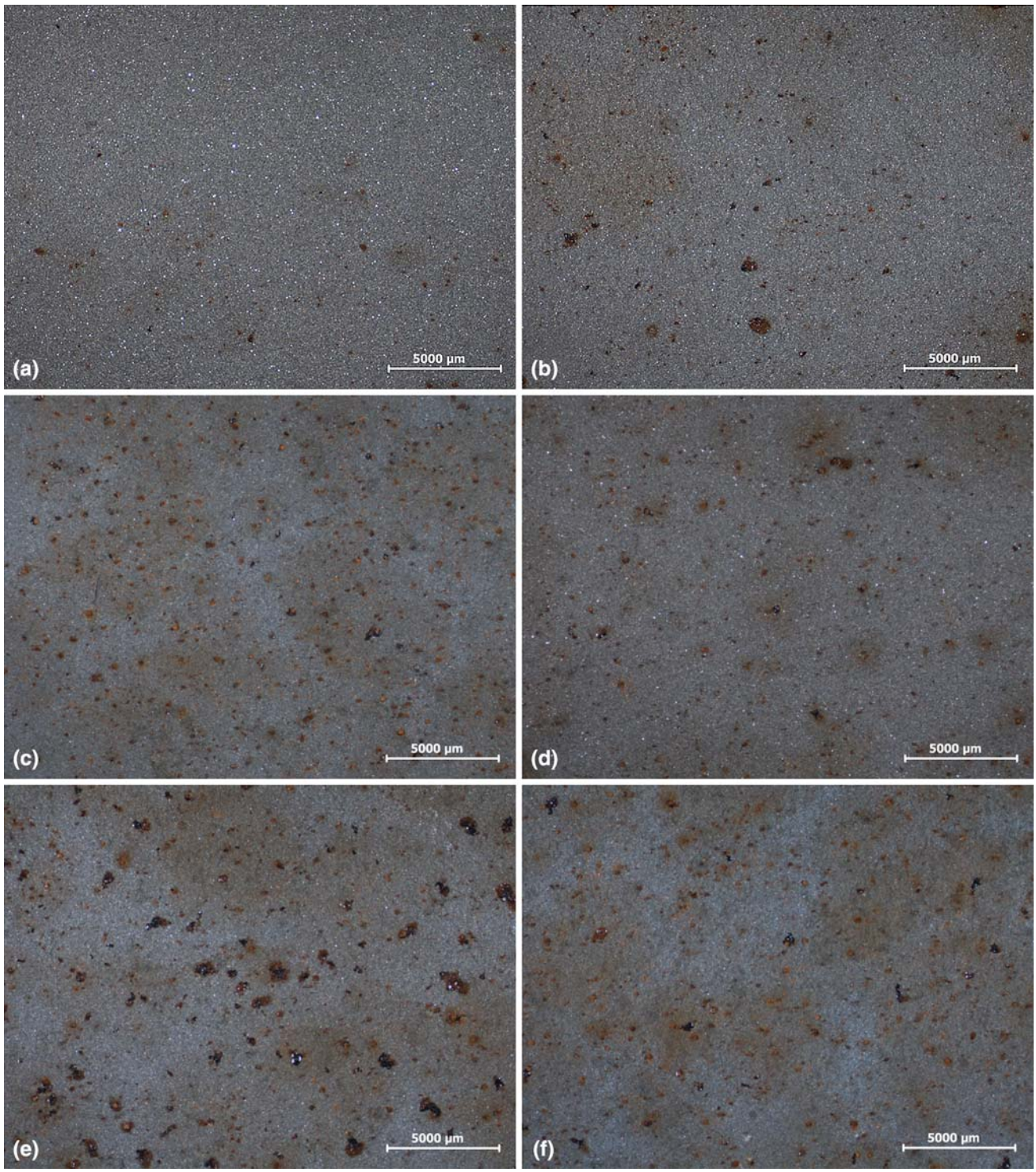

Fig. 6 Surface of CS (a) Ni-20Cr+50Al_2O_3 (−90 + 45 μm), (b) Ni-20Cr+50Al_2O_3 (−45 + 22 μm), (c) Ni-20Cr+50Al_2O_3 (−22 + 5 μm), (d) Ni-20Cr+30Al_2O_3 (−90 + 45 μm), (e) Ni-20Cr+30Al_2O_3 (−45 + 22 μm), and (f) Ni-20Cr+30Al_2O_3 (−22 + 5 μm) coatings after 48-h salt spray test, SM images

microstructural properties of the Ni-20Cr+Al_2O_3 coatings improved with the addition of Al_2O_3 particles together with high gas temperature. Their denseness improved noticeably with all compositions and particle sizes of Al_2O_3. However, because of a few weak spots, they lacked a fully dense microstructure. In this study, the Ni20-Cr+50Al_2O_3 (−90 + 45 μm) coating, though not even fully dense, was the most protective with the best impermeability with only a few pit-type corrosion spots detected on its surface.

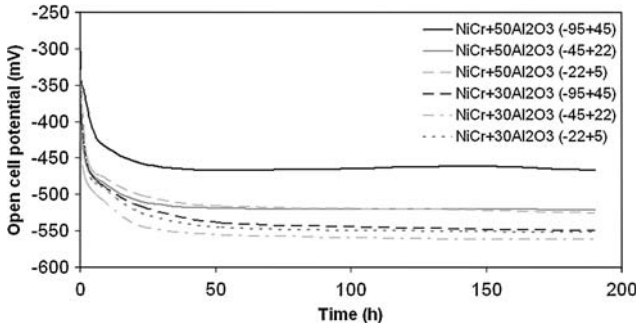

Fig. 7 Open-cell potential (vs. Ag/AgCl) of CS Ni-20Cr+Al_2O_3 coatings with 30% or 50% Al_2O_3 (Al_2O_3 particle sizes: $-90+45$ μm, $-45+22$ μm, and $-22+5$ μm) as a function of exposure time

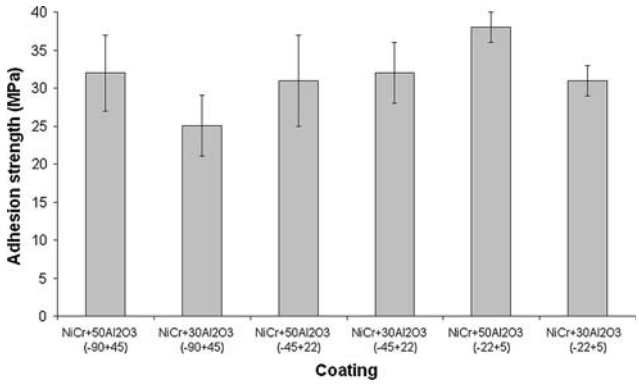

Fig. 8 Adhesion strengths (and standard deviations) of CS Ni-20Cr+Al_2O_3 coatings with 30% or 50% Al_2O_3 (Al_2O_3 particle sizes: $-90+45$ μm, $-45+22$ μm, and $-22+5$ μm)

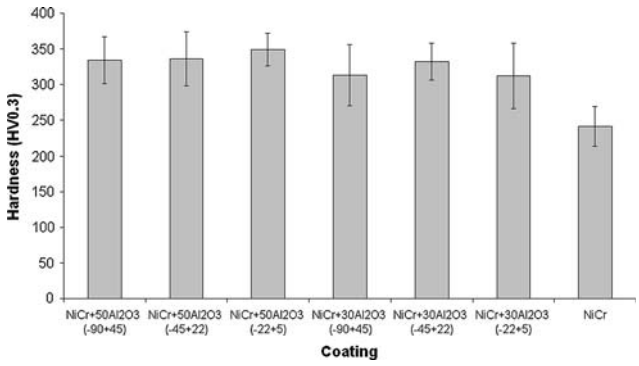

Fig. 9 Vickers hardness $HV_{0.3}$ (and standard deviations) of CS Ni-20Cr+Al_2O_3 coatings with 30% or 50% Al_2O_3 (Al_2O_3 particle sizes: $-90+45$ μm, $-45+22$ μm, and $-22+5$ μm) and CS Ni-20Cr coating

3.3 Mechanical Properties

The Ni-20Cr+Al_2O_3 coatings were tested for adhesion strength and hardness to obtain information on the effect of the Al_2O_3 particles on some mechanical properties. In a previous study (Ref 17), the adhesion strength of a Ni-20Cr coating on a steel substrate was 31 MPa, which was used as a reference in this study. The adhesion strength of Ni-20Cr+Al_2O_3 coatings is shown in Fig. 8. In the all cases, failure occurred at the interface between coating and substrate. The Ni-20Cr+Al_2O_3 coatings showed an adhesion strength of 25-38 MPa, whereas the Ni-20Cr+50Al_2O_3 ($-22+5$ μm) coating obtained the highest adhesion strength. The adhesion strengths of the Ni-20Cr+Al_2O_3 coatings were slightly higher than that of the Ni-20Cr coating depending on the composition. Because adding Al_2O_3 particles to the metallic Ni-20Cr powder only slightly affected the adhesion strength, it can conclude that in all cases, with and without an Al_2O_3 particles mixing, the adhesion strengths between the Ni-20Cr coatings and substrates were acceptable, indicating a reasonable adhesion between coatings and substrates.

Figure 9 shows the Vickers hardness ($HV_{0.3}$) of Ni-20Cr+Al_2O_3 and Ni-20Cr coatings. For the Ni-20Cr coating, it was 240 $HV_{0.3}$ and between 320 and 340 $HV_{0.3}$ for the Ni-20Cr+Al_2O_3 coatings. The Al_2O_3 particles affected the hardness by increasing its value, the effect arising from hardening by the hard particles. In addition to the effect of Al_2O_3 particles, high gas temperature affected the properties of coatings deposited. The effect of the Al_2O_3 addition on hardness was noticeable. In the hardness measurements, the indentations were taken in the metallic coating areas to evaluate the behavior of the metallic Ni-20Cr particles. The high hardness of the Ni-20Cr+Al_2O_3 coatings was reflected in their high work hardening (Ref 8). More hardening (compacting effect of Al_2O_3 particles) occurred at higher particle velocities (Ref 9) caused by the high gas temperature. Comparison of the Ni-20Cr and Ni-20Cr+Al_2O_3 coatings revealed that, the Al_2O_3 addition together with a high gas temperature had a pronounced effect on microstructural properties and on hardness values. A high hardness was caused by the work hardening of the particles together with high plastic deformation during impacts. On the other hand, the Al_2O_3 particles may also have reinforced the structure and thereby increased the hardness. In this study, the particle size and composition of Al_2O_3 had no clear effect on hardness.

4. Conclusions

Adding ceramic particles, in this study Al_2O_3, affected the properties of coating deposited by CS process. On the other hand, Al_2O_3 particles mixed with a metal alloy powder also had a technical spraying effect on the process parameters: they enabled the use of a higher gas temperature (700 °C) without clogging the nozzle. Adding Al_2O_3 powder affected mostly the microstructure. With the Al_2O_3 particles (high gas temperature) and compared to the Ni-20Cr coating, the metallic deposition buildup (coating thickness) of the Ni-20Cr+Al_2O_3 coatings increased. Their coating thickness increased with an increasing particle size and a decreasing composition of

Al_2O_3. The Ni-20Cr coating showed prevalent through-porosity, as demonstrated by corrosion products from the substrate on its surface after a salt spray test. The Al_2O_3 addition markedly affected the denseness of the Ni-20Cr+Al_2O_3 coatings with only a few pit-type corrosion spots visible on their surface. Obviously, the coatings did not have a fully, evenly dense structure, but they showed clear improvement. Moreover, adding Al_2O_3 particles decreased also the coatings' porosity in comparison with Ni-20Cr. The Al_2O_3 addition had a minor effect on the coatings' mechanical properties. The Ni-20Cr and Ni-20Cr+Al_2O_3 coatings showed reasonable adhesion strengths of about 30 MPa. The Al_2O_3 addition affected more the hardness of the coating's metallic part by increasing it, indicating reinforcement and high plastic deformation of the Ni-20Cr particles due to the high gas temperature.

Though high-pressure CS process uses mostly metallic powders, this study shows that metal alloy-ceramic powder blends could also be used. Generally, the composition of the powder depends on the properties desired for the coating. However, coating properties can be improved and spraying parameters extended by adding Al_2O_3 particles to Ni-20Cr powder. Furthermore, for pure Ni-20Cr coating, the powder must be optimized to make full use of a high gas temperature. The results of this study are promising, but for CS coatings, optimization of the powders and parameters is needed to produce fully, evenly dense coatings.

Acknowledgments

The authors like to thank Mr. Werner Krömmer of Linde AG Gas for the spray coatings and for his valuable advice. The project was funded by Finnish Funding Agency for Technology and Innovation (TEKES) and a group of Finnish industrial companies.

References

1. A. Papyrin, V. Kosarev, S. Klinkov, A. Alkimov, and V. Fomin, *Cold Spray Technology*, 1st ed., Elsevier, the Netherlands, 2007, p 328
2. T. Stoltenhoff, H. Kreye, and H.J. Richter, An Analysis of the Cold Spray Process and Its Coatings, *J. Therm. Spray Technol.*, 2001, **11**(4), p 542-550
3. T.H. Van Steenkiste, J.R. Smith, and R.E. Teets, Aluminum Coatings Via Kinetic Spray with Relatively Large Powder Particles, *Surf. Coat. Technol.*, 2002, **154**, p 237-252
4. C. Borchers, F. Gärtner, T. Stoltenhoff, H. Assadi, and H. Kreye, Microstructural and Macroscopic Properties of Cold Sprayed Copper Coatings, *J. Appl. Phys.*, 2003, **93**(12), p 10064-10070
5. R.G. Maev and V. Leshchynsky, Air Gas Dynamic Spraying of Powder Mixtures: Theory and Application, *J. Therm. Spray Technol.*, 2006, **15**(2), p 198-205
6. R.C. Dykhuizen and M.F. Smith, Gas Dynamic Principles of Cold Spray, *J. Therm. Spray Technol.*, 1998, **7**(2), p 205-212
7. H.C. Starck, Amperit and Amperweld Homepage, Amperit Thermal Spray Powders Procure. Available from http://www.amperit.info/index.php?page_id=2029
8. E. Calla, D.G. McCartney, and P.H. Shipway, Deposition of Copper by Cold Gas Dynamic Spraying: An Investigation of Dependence of Microstructure and Properties of the Deposits on the Spraying Conditions, *Thermal Spray 2004: Advances in Technology and Application*, 10-12 May, 2004 (Osaka, Japan), ASM International, p 6
9. T. Schmidt, F. Gärtner, and H. Kreye, New Developments in Cold Spray Based on Higher Gas- and Particle Temperatures, *J. Therm. Spray Technol.*, 2006, **15**(4), p 488-494
10. P. Richter and H. Höll, Latest Technology for Commercially Available Cold Spray Systems, *Thermal Spray 2006: Building on 100 Years of Success*, B.R. Marple, M.M. Hyland, Y.-C. Lau, R.S. Lima, and J. Voyer, Ed., May 15-18, 2006 (Seattle, Washington, USA), ASM International, p 3
11. H. Kreye, T. Schmidt, F. Gärtner, and T. Stoltenhoff, The Cold Spray Process and Its Optimization, *Thermal Spray 2006: Building on 100 Years of Success*, B.R. Marple, M.M. Hyland, Y.-C. Lau, R.S. Lima, and J. Voyer, Ed., May 15-18, 2006 (Seattle, Washington, USA), ASM International, p 5
12. B.B. Djordjevic and R.G. Maev, SIMAT™ Application for Aerospace Corrosion Protection and Structural Repair, *Thermal Spray 2006: Building on 100 Years Success*, B.R. Marple, M.M. Hyland, Y.C. Lau, R.S. Lima, and J. Voyer, Ed., May 15-18, 2006 (Seattle, Washington, USA), ASM International, p 5
13. A. Shkodkin, A. Kashirin, O. Klyuev, and T. Buzdygar, The Basic Principles of DYMET Technology, *Thermal Spray 2006: Building on 100 Years Success*, B.R. Marple, M.M. Hyland, Y.C. Lau, R.S. Lima, and J. Voyer, Ed., May 15-18, 2006 (Seattle, Washington, USA), ASM International, p 3
14. D. Helfritch, and V. Champagne, Optimal Particle Size for the Cold Spray Process, *Thermal Spray 2006: Building on 100 Years of Success*, B.R. Marple, M.M. Hyland, Y.-C. Lau, R.S. Lima, and J. Voyer, Ed., May 15-18, 2006 (Seattle, Washington, USA), ASM International, p 5
15. H. Mäkinen (Koivuluoto), J. Lagerbom, and P. Vuoristo, Mechanical Properties and Corrosion Resistance of Cold Sprayed Coatings, *Thermal Spray 2006: Building on 100 Years of Success*, B.R. Marple, M.M. Hyland, Y.-C. Lau, R.S. Lima, and J. Voyer, Ed., May 15-18, 2006 (Seattle, Washington, USA), ASM International, p 6
16. H. Koivuluoto, J. Lagerbom, and P. Vuoristo, Microstructural Studies of Cold Sprayed Copper, Nickel, and Nickel-30%Copper Coatings, *J. Therm. Spray Technol.*, 2007, **16**(4), p 488-497
17. H. Mäkinen (Koivuluoto), J. Lagerbom, and P. Vuoristo, Adhesion of Cold Sprayed Coatings: Effect of Powder, Substrate, and Heat Treatment, *Thermal Spray 2007: Global Coating Solutions*, B.R. Marple, M.M. Hyland, Y.-C. Lau, C.-J. Li, R.S. Lima, and G. Montavon, Ed., May 14-16, 2007 (Beijing, China), ASM International, p 31-36